Internal Medicine
The Japanese Society of Internal Medicine
doi: 10.2169/internalmedicine.7436-21
Intern Med 61: 1043-1048, 2022
http://internmed.jp

【 CASE REPORT 】

Primary Pulmonary Mucosa-associated Lymphoid Tissue Lymphoma with the High Expression of IgG4

Hiroki Tanahashi[1], Kakuhiro Yamaguchi[1], Tomoko Koura[1], Takahiro Kambara[2], Kyohei Yamada[3], Shinjiro Sakamoto[1], Yasushi Horimasu[1], Takeshi Masuda[1], Shintaro Miyamoto[1], Taku Nakashima[1], Hiroshi Iwamoto[1], Noriyasu Fukushima[4], Kazunori Fujitaka[1], Hironobu Hamada[1], Tatsuo Ichinohe[4], Koichi Ohshima[3] and Noboru Hattori[1]

Abstract:
This is the first report describing primary pulmonary mucosa-associated lymphoid tissue (MALT) lymphoma with the high expression of IgG4. The histological findings were compatible with the diagnostic criteria for MALT lymphoma and IgG4-related respiratory disease (IgG4-RRD). An unfixed sample for Southern blotting was not obtained since computed tomography findings showed multiple lung cysts, which is rare in patients with MALT lymphoma. However, polymerase chain reaction using paraffin sections showed the clonality of the immunoglobulin heavy chain variable region gene rearrangement, confirming a diagnosis of MALT lymphoma. This is an instructive case in which primary pulmonary MALT lymphoma was histologically compatible with IgG4-RRD.

Key words: pulmonary MALT lymphoma, IgG4, multiple lung cysts

(Intern Med 61: 1043-1048, 2022)
(DOI: 10.2169/internalmedicine.7436-21)

Introduction

Mucosa-associated lymphoid tissue (MALT) lymphoma is a low-grade B-cell lymphoma that occurs in various organs, including the stomach, lungs, salivary glands, orbits, and skin (1). It is known to develop against a background of chronic inflammatory conditions, such as the development of gastric MALT lymphoma in association with *Helicobacter pylori* infection (2). Some recent reports demonstrated the development of MALT lymphoma superimposed on IgG 4-related disease (IgG4-RD) or with the high expression of IgG4 in several organs, including the orbits and skin (3, 4). However, no previous report has described an association between IgG4 and primary pulmonary MALT lymphoma.

Primary pulmonary MALT lymphoma originates from bronchus-associated lymphoid tissue (BALT) and is relatively rare, representing <1% of lung tumors (5). It presents with a variety of shadows, typically consolidation, nodules, and ground glass shadows, on chest computed tomography (CT). Additionally, a few reports have described multiple cystic lesions as a rare CT finding of the disease (6, 7). The diagnosis of MALT lymphoma is generally established by identifying immunoglobulin gene rearrangement in Southern blotting using unfixed samples; however, polymerase chain reaction (PCR) using paraffin sections is also useful, especially when unfixed samples are not available (8, 9).

This report describes the first case of a primary pulmonary MALT lymphoma presenting with a high IgG4 expression level. Interestingly, the histological findings were compatible with the diagnostic criteria for MALT lymphoma and IgG4-related respiratory disease (IgG4-RRD) (10). Because of the presence of clonal gene rearrangement of immunoglobulin heavy chain variable region (IgVH) in PCR using

[1]Department of Respiratory Medicine, Hiroshima University Hospital, Japan, [2]Department of Pathology, Hiroshima University Graduate School of Biomedical and Health Science, Japan, [3]Department of Pathology, Kurume University School of Medicine, Japan and [4]Department of Hematology, Hiroshima University Hospital, Japan
Received: February 26, 2021; Accepted: August 5, 2021; Advance Publication by J-STAGE: September 18, 2021
Correspondence to Dr. Kakuhiro Yamaguchi, yamaguchikakuhiro@gmail.com

paraffin sections, the patient was diagnosed with MALT lymphoma. This is an instructive case, suggesting a potential association between the expression of IgG4 and the pathogenesis of primary pulmonary MALT lymphoma.

Case Report

The patient was a 53-year-old woman who initially visited a local hospital for the evaluation of abnormal shadows on a chest radiograph. She underwent chest CT, which showed multiple lung cysts, ground glass shadows, and nodules. Therefore, she was referred to our hospital. The patient had no symptoms, including fever and dyspnea. She was an ex-smoker (2.5 pack-years, until 30 years of age). She had glaucoma but had never taken any drugs. She was an office worker and did not have any relevant family history or allergic diseases. Oxygen desaturation was not observed, and no abnormalities were found on a physical examination. Chest radiography did not show any obvious abnormal findings (Fig. 1). However, chest CT revealed multiple thin-walled cysts, ground glass shadows, and nodules, without evidence of mediastinal lymphadenopathy (Fig. 2). Fluorodeoxyglucose-positron emission tomography (FDG-PET) showed that the maximal standardized uptake value of the nodule in the right S7 was 3.5 (Fig. 3).

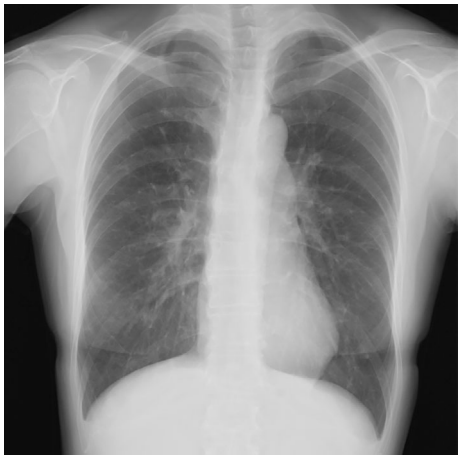

Figure 1. A chest radiograph obtained at the first visit. The radiograph did not show any obvious abnormal findings.

We suspected lung cancer, granulomatous polyangiitis, pulmonary lymphangioleiomyomatosis, and lymphocytic interstitial pneumonia (LIP) associated with Sjögren's syndrome based on the CT findings. Blood tests were performed for the differentiation of these conditions; however, no obvious abnormalities were found, with the exception of mild elevation of the alanine transaminase level (Table). The levels of anti-nuclear antibodies, anti-SS-A/B antibodies, anti-neutrophil cytoplasmic antibodies, and tumor markers including soluble interleukin-2 receptor were within their respective normal ranges. Additionally, this patient was not suffering from ocular or oral dryness; thus, Sjögren's syndrome and Sjögren's syndrome-associated LIP were ruled out.

Flexible bronchoscopy was performed for histological diagnosis. Bronchoalveolar lavage fluid was obtained, and the total cell count was normal (8.98×10^4/mL; macrophages:

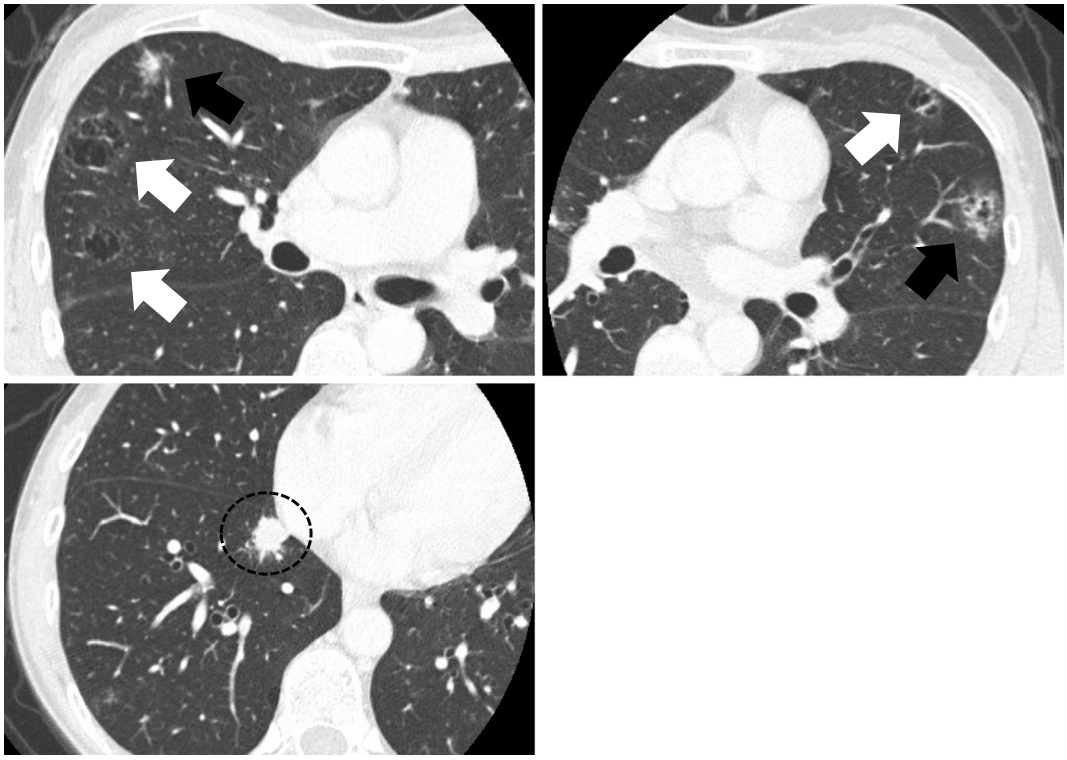

Figure 2. A chest computed tomography (CT) scan obtained at the first visit. CT showed multiple thin-walled cysts (white arrows), ground glass shadows (black arrows), and a nodule (dotted circle).

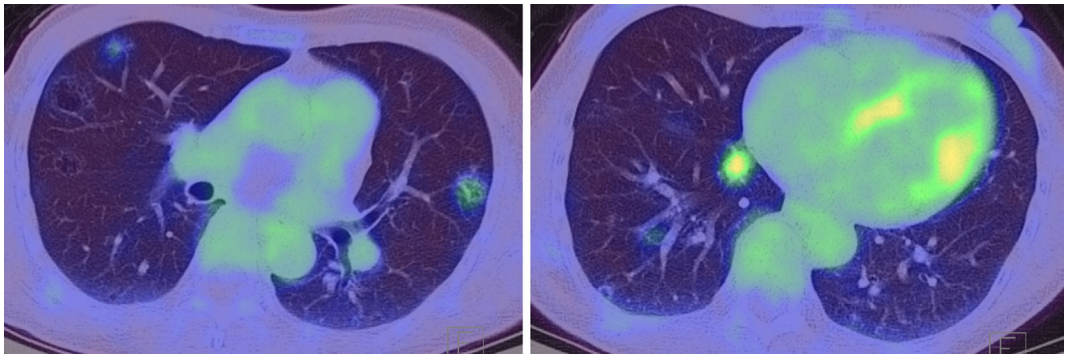

Figure 3. **A fluorodeoxyglucose-positron emission tomography (FDG-PET) scan obtained before admission. FDG-PET showed the increased uptake of FDG. The maximal standard uptake value of the nodule in the right S7 was 3.5, while the values of other areas were up to 1.5.**

Table. **Laboratory Findings at the First Visit.**

Hematology		Biochemistry			
WBC	7,930 /μL	TP	7.4 g/dL	KL-6	268 IU/mL
Neut	72.1 %	Alb	4.3 g/dL	ANA	×80
Lymp	22.4 %	AST	23 IU/L	Anti SS-A	1.9 IU/mL
Mono	4.5 %	ALT	45 IU/L	Anti SS-B	<1.0 IU/mL
Eos	0.9 %	T-bil	136 mg/dL	PR3-ANCA	<1.0
RBC	4.89×10^6 /μL	LDH	136 IU/L	MPO-ANCA	<1.0
Hb	13.8 g/dL	γ-GTP	61 IU/L	IgG	1,331 mg/dL
PLT	35.8×10^4 /μL	BUN	20 mg/dL	IgG4	70.3 mg/dL
		Cre	0.56 mg/dL	IgA	163 mg/dL
		Glu	110 mg/dL	IgM	162 mg/dL
		Na	139 mEq/L		
		K	4.6 mEq/L	Tumor marker	
		Cl	104 mEq/L	Pro-GRP	52.5 pg/mL
		Ca	9.6 mg/dL	CEA	1.2 ng/dL
		CRP	0.02 mg/dL	CYFRA	1.5 ng/dL
				sIL-2R	347 IU/mL

WBC: white blood cells, Neut: neutrophils, Lymp: lymphocytes, Mono: monocytes, Eos: eosinophils, RBC: red blood cells, Hb: hemoglobin, PLT: platelets, TP: total protein, Alb: albumin, AST: aspartate transaminase, ALT: alanine transaminase, T-bil: total bilirubin, LDH: lactate dehydrogenase, γ-GTP: gamma glutamyltransferase, BUN: blood urea nitrogen, Cre: creatinine, Glu: glucose, Na: sodium, K: potassium, Cl: chlorine, Ca: calcium, CRP: C-reactive protein, KL-6: Krebs von den Lungen 6, ANA: antinuclear antibody, SS: Sjögren's syndrome, PR3: proteinase 3, ANCA: antineutrophil cytoplasmic antibody, MPO: myeloperoxidase, Ig: immunoglobulin, GRP: gastrin releasing peptide, CEA: carcinoembryonic antigen, CYFRA: cytokeratin fragment, sIL: soluble interleukin

84.8%, lymphocytes: 15.9%, neutrophils: 0.3%, eosinophils: 0.0%, CD4/CD8: 1.31). Transbronchial lung biopsies showed no specific findings. Therefore, thoracoscopic partial resection of nodules in right S7 and S10 was performed.

The histopathological examination of the specimens revealed the diffuse infiltration of lymphocytes with poor atypia and plasma cells, follicular colonization, and the presence of lymphoepithelial lesions (Fig. 4A, B). Although the histological findings were consistent with multicentric Castleman disease, the clinical diagnostic criteria were not met because of the absence of lymphadenopathy, elevation of inflammatory markers, and hepatosplenomegaly. The lymphocytes were immunohistochemically positive for CD20 and CD79, and negative for CD3, CD5, and CD10 (Fig. 4C, D). These findings were compatible with MALT lymphoma. However, marked lymphocytic infiltration into the stroma of the peribronchovascular sheath and the interlobular septal wall, obliterative vasculitis, and storiform-like fibrosis were also seen (Fig. 4E, F). These findings suggested IgG4-RRD, and therefore, immunostaining for IgG4 was additionally performed. Although IgG4-positive plasma cells were sparse in the germinal center, the number of IgG4-positive plasma cells was 130/high-power field (HPF), and the IgG4/IgG-positive cell ratio was 60% (Fig. 4G, H). These histological findings were also compatible with the diagnostic criteria for IgG4-RRD (10), although there were no typical findings of IgG4-RD in the serum IgG4 level, lung tissue other than MALT lymphoma, or the extra-thoracic organs. MALT lym-

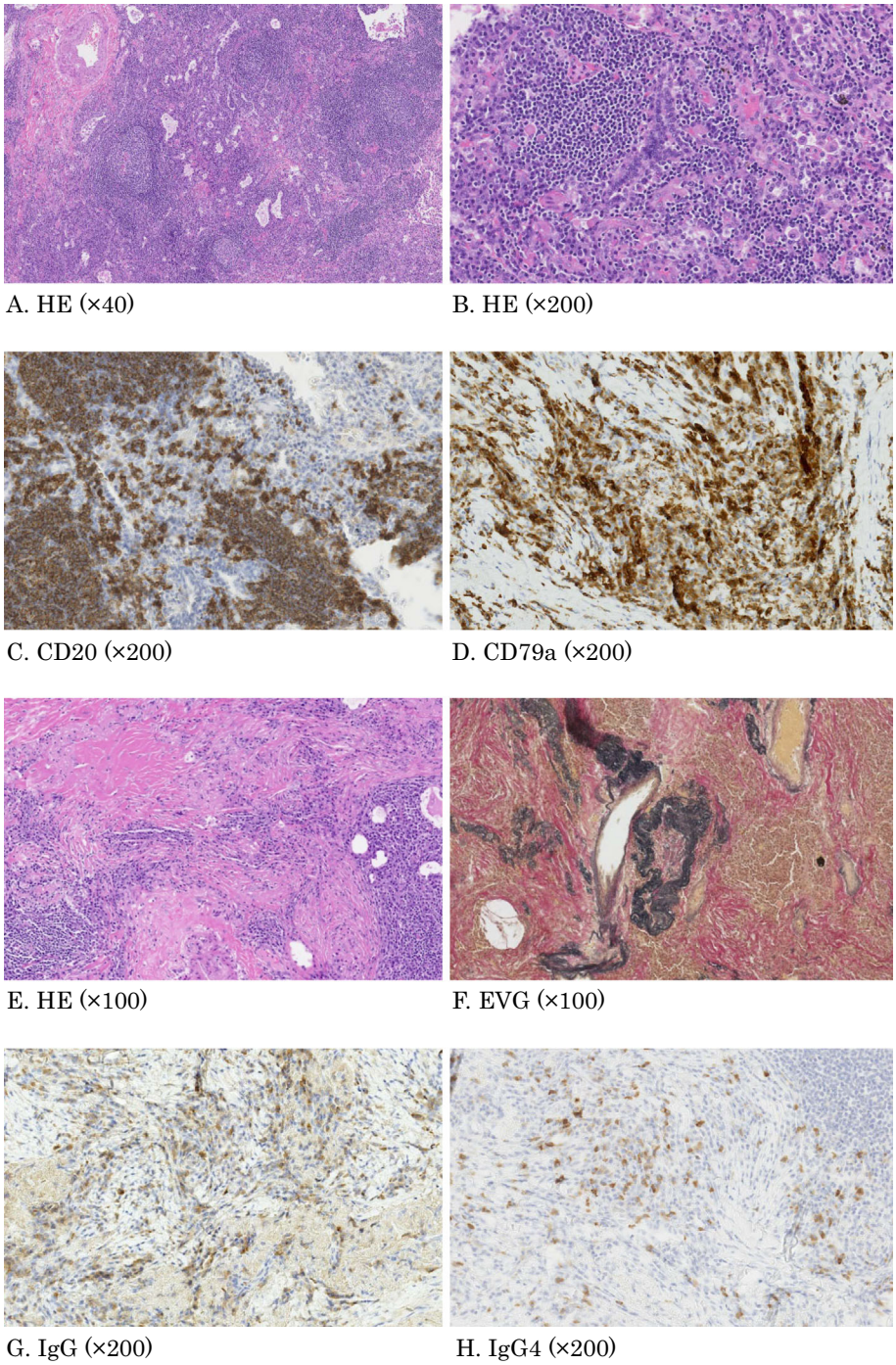

Figure 4. Histopathological and immunohistochemical findings of the specimen obtained from the lower lobe of the right lung (S7) by surgical biopsy. (A, B) Hematoxylin and Eosin (H&E) staining showing the diffuse infiltration of lymphocytes with poor atypia around bronchovascular bundles and bronchioles, follicular colonization, and lymphoepithelial lesions (A: H&E staining, ×40; B: H&E staining, ×200). (C, D) Immunohistochemical staining demonstrating that the lymphocytes were positive for CD20 and CD79a (C: CD20, ×200; D: CD79a, ×200). (E) H&E staining showing storiform-like fibrosis. (H&E staining, ×100). (F) Elastica van Gieson (EVG) staining showing obliterative vasculitis (EVG, ×100). (G, H) Immunohistochemical staining for IgG and IgG4. The number of IgG4-positive plasma cells was 130/high-power field (HPF), and the IgG4/IgG-positive cell ratio was 60% (G: IgG, ×200; H: IgG4, ×200). IgG4-positive plasma cells were mainly observed around the lymphoid follicle.

phoma can be differentiated from IgG4-RRD, by analyzing B-cell clonality. However, since the CT findings of the lung showed multiple cystic lesions, which are rare in patients with MALT lymphoma, an unfixed sample was not retained for Southern blotting. Therefore, PCR was performed using paraffin sections, which revealed the clonality of IgVH

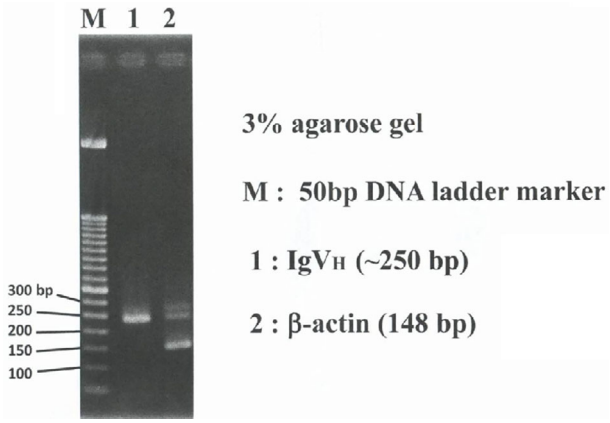

Figure 5. The PCR analysis of immunoglobulin heavy chain variable region (IgVH) gene rearrangement using paraffin sections revealed the clonality of IgVH.

(Fig. 5). Thus, we diagnosed primary pulmonary MALT lymphoma. Since the patient was asymptomatic, she was kept under observation.

Discussion

This is the first report describing primary pulmonary MALT lymphoma with histopathological features consistent with IgG4-RRD. The association between MALT lymphoma and IgG4-positive plasma cells is still unclear. One possible mechanism is the stromal infiltration of IgG4-positive plasma cells resulting in morphological changes similar to IgG4-RRD. Fujimoto et al. reported six cases of non-small cell lung cancer that met the histological criteria for IgG4-RRD, although none met the diagnostic criteria for IgG4-RD (11). Another possibility is that IgG4-RD could progress to MALT lymphoma, because several reports have shown that orbital MALT lymphoma develops superimposed on IgG4-RD (4, 12). Additionally, IgG4-RD has been reported to elevate the incidence of malignancies (13, 14). In this case, the serum levels of IgG4 were within the normal range, and no systemic manifestations of IgG4-RD were observed in the non-neoplastic lung tissue or extra-thoracic organs. Additionally, only a few IgG4-positive plasma cells were observed in the germinal center of the MALT lymphoma. These findings suggest that IgG4-positive plasma cells may infiltrate the stromal tissue of the MALT lymphoma resulting in histological changes similar to IgG4-RRD; however, further investigations are needed to determine the association between the high expression of IgG4 and pulmonary MALT lymphoma.

Primary pulmonary MALT lymphoma shows a variety of shadows; however, cysts are rare. Two factors may be responsible for the development of cysts. One is the MALT lymphoma itself. Pulmonary MALT lymphoma originates from BALT, which is found along the bifurcations of the upper bronchi, directly beneath the epithelium. Additionally, a previous study showed that the proliferation of BALT resulted in lower respiratory tract obstruction (15). These observations suggest that proliferated BALT might act as a check valve followed by cystic changes via overinflation of the alveoli. Another possibility is that the cysts that develop in patients with primary pulmonary MALT lymphoma are associated with an underlying collagen disease. Noguchi et al. reviewed eight patients with primary pulmonary MALT lymphoma who presented with cystic abnormalities and reported that three of them had Sjögren's syndrome as an associated comorbidity. Multiple lung cysts are a common manifestation in patients with Sjögren's syndrome (7). However, our patient did not present with Sjögren's syndrome. These data suggest that MALT lymphoma itself contributed to the development of the lung cysts in this case, although further investigations are needed to elucidate the mechanisms underlying the development of lung cysts in pulmonary MALT lymphoma.

In this case, primary pulmonary MALT lymphoma was diagnosed on the basis of monoclonal IgVH gene rearrangement by PCR using paraffin sections. Southern blotting with unfixed samples is the gold standard method for identifying the clonality of immunoglobulin gene rearrangement. Nevertheless, PCR is also useful because it has higher sensitivity than Southern blotting and therefore paraffin sections can be used for the detection of clonality (9). In this case, the possibility of a primary pulmonary MALT lymphoma was not considered before surgical lung biopsy because of the rare CT findings; thus, unfixed specimens were not retained for Southern blotting. In such situations, PCR can be performed using paraffin sections to detect clonality and additional biopsy can be avoided.

Conclusion

This is the first case of primary pulmonary MALT lymphoma with histopathological features consistent with IgG4-RRD. This report suggests a potential association between IgG4 and primary pulmonary MALT lymphoma.

The authors state that they have no Conflict of Interest (COI).

References

1. Isaacson PG, Spencer J. Malignant lymphoma of mucosa-associated lymphoid tissue. Histopathology **11**: 445-462, 1987.
2. Zucca E, Bertoni F. The spectrum of MALT lymphoma at different sites: biological and therapeutic relevance. Blood **127**: 2082-2092, 2016.
3. Bledsoe JR, Wallace ZS, Stone JH, Deshpande V, Ferry JA. Lymphomas in IgG4-related disease: clinicopathologic features in a western population. Virchows Arch **472**: 839-852, 2018.
4. Cheuk W, Yuen HK, Chan AC, et al. Ocular adnexal lymphoma associated with IgG4+ chronic sclerosing dacryoadenitis: a previously undescribed complication of IgG4-related sclerosing disease. Am J Surg Pathol **32**: 1159-1167, 2008.
5. Cadranel J, Wislez M, Antoine M. Primary pulmonary lymphoma. Eur Respir J **20**: 750-762, 2002.
6. Bae YA, Lee KS, Han J, et al. Marginal zone B-cell lymphoma of bronchus-associated lymphoid tissue: imaging findings in 21 pa-

tients. Chest **133**: 433-440, 2008.
7. Noguchi S, Yatera K, Kido T, et al. Pulmonary mucosa-associated lymphoid tissue (MALT) lymphoma with multiple thin-walled pulmonary cysts: a case report and review of the literature. Intern Med **52**: 2325-2329, 2013.
8. Svachova M, Tichy M. PCR analysis of immunoglobulin heavy chain and TCR gene rearrangements in diagnosis of lymphoproliferative disorders on formalin-fixed, paraffin-embedded tissues. Neoplasma **55**: 36-41, 2008.
9. Medeiros LJ, Carr J. Overview of the role of molecular methods in the diagnosis of malignant lymphomas. Arch Pathol Lab Med **123**: 1189-1207, 1999.
10. Matsui S, Yamamoto H, Minamoto S, Waseda Y, Mishima M, Kubo K. Proposed diagnostic criteria for IgG4-related respiratory disease. Respir Investig **54**: 130-132, 2016.
11. Fujimoto M, Yoshizawa A, Sumiyoshi S, et al. Stromal plasma cells expressing immunoglobulin G4 subclass in non-small cell lung cancer. Hum Pathol **44**: 1569-1576, 2013.
12. Sato Y, Ohshima K, Ichimura K, et al. Ocular adnexal IgG4-related disease has uniform clinicopathology. Pathol Int **58**: 465-470, 2008.
13. Yamamoto M, Takahashi H, Tabeya T, et al. Risk of malignancies in IgG4-related disease. Mod Rheumatol **22**: 414-418, 2012.
14. Asano J, Watanabe T, Oguchi T, et al. Association between immunoglobulin G4-related disease and malignancy within 12 years after diagnosis: an analysis after longterm followup. J Rheumatol **42**: 2135-2142, 2015.
15. Kinsely BL, Mastey LA, Mergo PJ, et al. Pulmonary mucosa-associated lymphoid tissue lymphoma: CT and pathologic findings. AJR Am J Roentgenol **172**: 1321-1326, 1999.